Soft- and Hard-Segment Phase Segregation of Polyester-Based Polyurethane

Kun-San Chen[1], T. Leon Yu[1,*], Yung-Sin Chen[1], Tsang-Lang Lin[2] and Wen-Jiun Liu[2]

1. *Department of Chemical Engineering, Yuan-Ze University, Taoyuan, Nei-Li 32026, Taiwan*
2. *Department of Engineering and System Science, National Tsing-Hua University, Hsinchu 30043, Taiwan*

Received November 10, 2000; revised February 9, 2001; accepted March 15, 2001.

Abstract: Polyester based polyurethanes were synthesized from 4,4'-methylene bis(phenyl isocyanate) (MDI) with butanediol as a chain extender and low molecular weight polyester-diol as a soft segment. Three polyesters were used in the synthesis of polyurethanes. Two of the polyesters, with molecular weight M_n = 2,660 and 2,155, were synthesized from adipic acid and 1,6-hexanediol, which had an even number of carbon atoms (polyester-6-6-1 and polyester-6-6-2). The other polyester with M_n = 2,770 was synthesized from pimelic acid and 1,5-pentanediol, which had an odd number of carbon atoms (polyester-7-5). Polyester-6-6-1 and polyester-6-6-2 consisting of even carbon monomers, had a higher degree of crystallinity at room temperature than polyester-7-5, which consists of an odd number of carbon monomers. The effect of polyester molecular weight and soft and hard-segmental geometric structure on the soft- and hard-segmental phase segregation was studied using differential scanning calorimetry (DSC), Fourier transform infrared spectroscopy (FTIR), and small angle X-ray scattering (SAXS).

Keywords: Polyurethane, Phase segregation, DSC, FTIR, SAXS.

Introduction

The segmented polyurethanes are thermoplastic elastomers with high elongation characteristics, along with typical properties of plastics such as modulus, strength, and processibility. It is generally agreed that the unique mechanical properties of polyurethanes, as compared to other types of elastomers, are predominantly controlled by the microphase structure resulting from the incompatibility of the soft and hard segments [1,2]. This incompatibility of the soft and hard segments leads to a phase separation which is reflected in a rubber-like matrix containing hard microdomains. The mechanical strength in this structure can be attributed to the hard microdomains cross-linked through H-bonding which act as rigid reinforcing particles.

The polyester based urethanes consist of an aromatic diisocyanate with a glycol chain extender as the hard segment and a low molecular weight polyester as the soft segment. They are considered to be linear segmented block copolymers made up of alternating hard and soft block segments. Compositional variables and processing conditions are known to affect the degree of phase segregation, phase mixing, hard segment domain organization, and subsequent polyurethane properties [2-4]. Depending on the relative incompatibility of the hard and soft segments, phase segregation will occur during processing and post cure annealing. The effects of polyurethane composition and structure on the resultant properties has been investigated by several researchers [5-31]. These studies have concentrated on model compounds based on aromatic diisocyanates, such as toluene diisocyanate (TDI) [5,6] or 4,4'-methylene bis(phenyl isocyanate) (MDI) [5-8]. The phase segregation of hard and soft segment domains has been demonstrated by small and wide angle X-ray scattering [9-22], differential scanning calorimetry (DSC) [9-18,23-26], infrared spectroscopy (IR) [26-

*To whom all correspondence should be addressed.
Tel: 886-3-4638800 ext 553; Fax: 886-3-4559373
E-mail: cetlyu@saturn.yzu.edu.tw

J. Polym. Res. is covered in ISI (CD, D, MS, Q, RC, S), CA, EI, and Polymer Contents.

31], microscopy [16,32,33], small angle laser light scattering (SALS) [16], and dynamic mechanical thermal analysis (DMTA) [18].

In our previous work [34], the effect of soft segment polyester $-CH_3$ side chain content on hard and soft segment phase segregation was studied by DSC and small angle X-ray scattering (SAXS). The experimental data revealed that the hard segment ordering domain and the degree of soft- and hard- segment phase segregation of polyurethane increased with the polyester $-CH_3$ side chain content. It has been reported that soft- and hard segmental phase segregation of polyurethanes is strongly controlled by the compatibility of these two segments and the chain mobility of hard segments inside the soft domain [14,35]. Since increasing the polyester $-CH_3$ side chain leads to an increase in the free volume of the soft segment domain and thus a higher mobility of hard segment molecules inside the soft domain, we believed that the free volume of the polyester soft domain strongly affected the soft- and hard-segment phase segregation.

With polyurethanes of structure $-[(O=C)NH-(CH_2)_nNH(C=O)O(CH_2)_mO]-$, it has been shown that when "*n*" and "*m*" are even, the fit of each hydrogen donor group (NH) to each electron donor group (C=O) should be relatively easy, whereas when "*n*" or "*m*" is odd, the fit should not be perfect [36]. Thus, in an irregular structure (when *n* or *m* is odd and the fit is poor) not all groups should participate in hydrogen bonding, inter-molecular attractions should be weaker, and the melting point should be lower.

It is known that the "*zig-zag*" structure of polyester affects the geometric fit of polymer molecules and thus the crystallization behavior of polyesters. A commercially important class of polyurethanes is those consisting of polyester as soft segments and MDI chains extended with 1,4-butanediol as hard segments. In the present work, we studied the soft- and hard- segment phase segregation behavior of polyester based-polyurethanes with two polyurethanes (PU-6-6-1 and PU-6-6-2) having polyesters synthesized from even carbon monomers, i.e., adipic acid and 1,6-hexanediol (polyester-6-6) and the other polyurethane (PU-7-5) having polyester synthesized from odd carbon monomers, i.e., pimelic acid and 1,5-pentanediol (polyester-7-5). DSC, FTIR, and SAXS measurements were carried out in this study. DSC provides the data for soft segment T_g, melting points as well as enthalpies of fusion of both the soft- and hard-segmental crystalline domains. FTIR provides information on hard segment hydrogen bonding. SAXS provides the long period (or inter-domain spacing) of repeat structures.

Figure 1 shows the geometric structures of hard segments, polyester-6-6, and polyester-7-5. All of the PUs used in this work had hard segments consisting of MDI and 1,4-buatnediol, which has an even number of carbon atoms. From Figure 1, it is obvious that the hard segments had a better geometric fit with polyesters consisting of even carbon monomers than with those consisting of odd carbon monomers. Polyesters made up of even carbon monomers should have a better geometric fit with each other and a higher degree of crystallinity than those made up of odd carbon monomers. Since the repeat units of polyester-6-6 and polyester-7-5 had same molar fraction of the –COO group, these two polyesters should have the same solubility parameters. The compatibility of the PU hard segments with the soft segments should be similar for all of the PUs. Under the same processing conditions and thermal history, the morphology of PUs depends on (1) the polyester soft segmental molecular weights, (2) the geometric fits of soft-to-soft segments and hard-to-soft segments, and (3) the mobility of polyurethane hard segments inside the polyester soft domains.

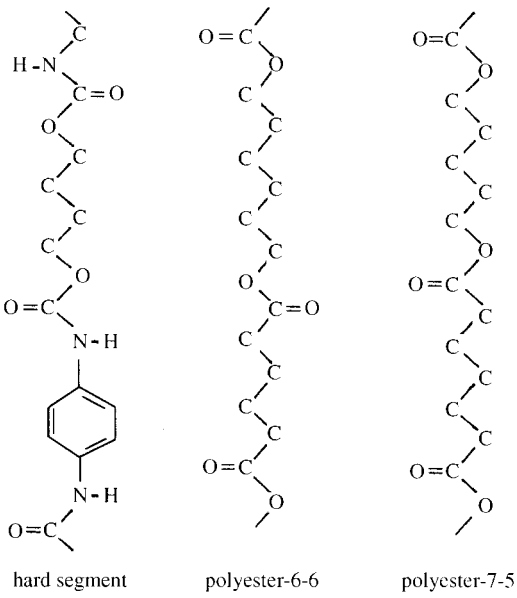

Figure 1. Geometric structure of (a) "MDI+1,4-butanediol" hard-segments, (b) polyester-6-6, and (c) polyester-7-5.

Experimental

1. Polyester-diol

Three polyesters were synthesized using a conventional method. Two of the polyesters (polyester-6-6-1 and polyester-6-6-2) consisted of 1,6-hexanediol and adipic acid (Riedel-de Haen Co) and the other (polyster-7-5) consisted of 1,5-pentanediol and pimelic acid (Riedel-de Haen Co) with

Table I. Chemical compositions and molecular weights of polyesters.

Sample	Polyester 6-6-1	Polyester-6-6-2	Polyester 7-5
Adipic acid (mole)	1.00	1.00	----
1,6-Hexaneanediol (mole)	1.19	1.21	----
Pimelic acid (mole)	----	----	1.00
1,5-Pentanediol (mole)	----	----	1.19
Acid value (mg KOH/g)	3.81	3.9	3.60
OH value (mg KOH/g)	42.1	43.2	40.5
M_n	2,660	2,155	2,770
M_w/M_n	1.81	1.95	1.84

Table II. Chemical compositions of polyurethanes.

Polyurethane[a]	Polyester (mole)	MDI (mole)	Butanediol (mole)	Soft-segment content (wt%)
PU-6-6-1	0.13	1.05	0.87	50.4
PU-6-6-2	0.16	1.05	0.84	50.5
PU-7-5	0.13	1.05	0.87	51.4

(a) The polyurethanes were synthesized from polyesters which have the same designated numbers as shown in Table I.

OH/COOH mole ratios around 1.19/1-1.21/1 under a nitrogen atmosphere. The chemical compositions of these three polyesters are listed in Table I. The reaction temperature was increased by stepwise control as follows: 140 °C/1 h, 150 °C/1 h, 160 °C/1 h, 180 °C/2 h, and 200 °C/4 h. The acid and –OH values of the final polyesters, determined by methods ASTM D4262 and D4274, respectively, are listed in Table I. The molecular weight distributions were determined by GPC (Waters model 746) with three Waters μ-styragel columns which had molecular weight ranges of 0-103, 102-5×10^3, and 5×10^2-2×10^4, and a RI detector at 25 °C. Tetrahydrofuran (THF, Merck Co) was used as the mobile phase, and narrow MWD polystyrene standards (Aldrich Chemical Co) were used in a linear calibration. The M_n and M_w of these polyesters are also listed in Table I.

2. Polyurethane

The polyester-diols synthesized from an experimental procedure (a) were used to synthesize polyurethanes with MDI (Tokyo Kasei Kogyo Co) and 1,4-butanediol (Riedel-de Haen Co) as a chain extender by the prepolymerization method. The chemical compositions of these polyurethanes are shown in Table II. Thus two of these polyurethanes (PU-6-6-1 and PU-6-6-2) had polyester soft segments consisting of even carbon monomers whilst the other polyurethane (PU-7-5) had a polyester soft segment consisting of odd carbon monomers. Polyester-diol was first reacted with diisocyanate at 90-100 °C for one hour in *N,N*-dimethyl formamide (DMF, Merck Co). The prepolymer was then reacted with 1,4-butanediol at 90-100 °C for another hour in DMF. The final polymer was then precipitated from methanol and the residual solvent was removed under a vacuum at 60 °C for 24 h. The polymer was then compression molded on a press at 225 °C for 3 min followed by cooling at an ambient temperature and environment. The samples were then kept at room temperature for at least one week before DSC, FTIR, and SAXS measurements were conducted. Before polymerization, the polyester was dried at 90 °C under a vacuum for 2 hour to remove moisture, and 1,4-butanediol and DMF were treated with a molecular sieve (Merck, pore size 0.4 nm) drying agent. MDI was used as received without further purification. The final polyurethane contained ~51.0 wt% of polyester.

3. Differential scanning calorimetry (DSC)

DSC measurements were carried out on a Du Pont 910 DSC. The heating rate was 10 °C/min for the temperature range of 100-300 °C. The sample sizes were around 10 mg for all measurements. Temperature calibration was done with a multiple indium-lead-nickel standard, and an indium standard was used for heat flow calibration.

4. Small angle X-ray scattering (SAXS)

SAXS measurements were performed with a pinhole collimated X-ray camera. The radiation source was a Rigaku 18 KW rotating anode generator with a Cu targe operated at 100 mA and 40 KeV (installed at the Department of Engineering and System Science, National Tsing-Hua University, Taiwan). A three-pinhole system was used to collimate the X-ray beams along with a graphite monochromator to control the incident X-ray beams on the sample. The scattered intensity was detected by a two-dimension multi-wire detector (Oak Ridge De-

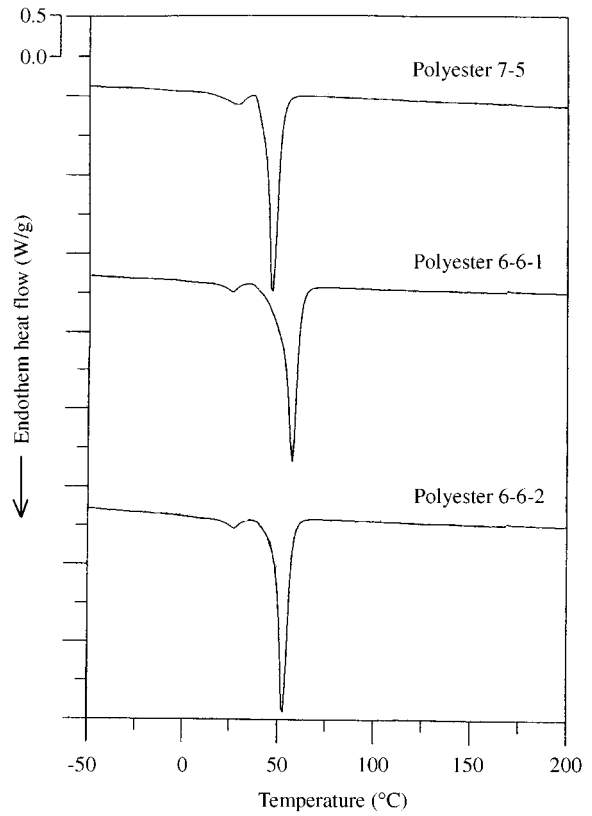

Figure 2. DSC curves of Polyester-7-5, Polyetser-6-6-1, and Polyester-6-6-2.

tector Laboratory, Inc.) with 256×256 channels for a 20 cm × 20 cm active area (1 mm between each pixel). The sample to detector distance was 500 cm in length. All data were corrected for background (dark current) and the sensitivity of each pixel in the area detector.

Results and Discussion

1. DSC study

1.1 DSC study of polyesters

Aliphatic linear polyesters behave as crystalline polymers at room temperature. The DSC curves (Figure 2) with a heating rate of 10 °C/min showed a small endothermic $\Delta H(I)$ at a lower melting temperature $T_m(I)$ and a large endothermic $\Delta H(II)$ at a higher melting temperature $T_m(II)$. The positions of the DSC endothermic peaks and heat of fusion of polyester-6-6-1, polyester-6-6-2, and polyester-7-5 are listed in Table III. After polymerization, these polyesters were stored at room temperature at least one week before DSC measurements were conducted. The uncertainty with each temperature was approximately ±1 °C. It is obvious that polyester-6-6-1 and polyester-6-6-2, which consist of monomers of even carbons, have higher $T_m(II)$ and $\Delta H(II)$ than polyester-7-5, which consists of monomers of odd carbons. These DSC results suggest that polyester-6-6-1 had the highest degree of crystallinity and polyester-7-5 had the lowest. Since polyester-6-6-1 and polyester-7-5 had similar molecular weight distributions, the difference in crystallization behavior between these two polyesters could be due to different "*zig-zag*" chemical structural conformations. The polyesters consisting of even carbon monomers had a better molecular geometric fit than those consisting of odd carbon monomers [36]. The DSC data also showed that polyester-6-6-1 had higher $T_m(II)$ and $\Delta H_m(II)$ than polyester-6-6-2 due to the higher molecular weight of polyester-6-6-1.

Table III. DSC data of polyesters.

Polyester	Polyester-6-6-1	Polyester-6-6-2	Polyester-7-5
T_{m1}(I-peak) (°C)	26	27	29
ΔH_1(I) (J/g)	4.8	5.4	8.9
T_{m1}(II-peak) (°C)	57	52	46
ΔH_1(II) (J/g)	107.4	101.5	92.5

Table IV. DSC data of polyurethanes annealed at room temperature.

Polyurethane[a]	PU-6-6-1	PU-6-6-2	PU-7-5
T_{g1} (°C)	-33	-38	-44
T_{m1} (I-peak) (°C)	19		22
T_{m1} (II-peak) (°C)	46	43	
ΔH_{m1} (I+II) (J/g)	34.8	2.0	4.2
T_{m2} (I-peak) (°C)		71	66
ΔH_{m2} (I) (J/g)		2.1	3.2
T_{m2} (II-peak) (°C)	158	162	162
ΔH_{m2} (II) (J/g)	3.2	8.6	9.6
T_{m2} (III-a-peak) (°C)			185
T_{m2} (III-b-peak) (°C)			198
ΔH_2 (III) (J/g)			9.4

(a) The subscripts 1 and 2 correspond to soft and hard segments, respectively.

1.2 DSC study of polyurethanes

DSC heating curves of PU-7-5, PU-6-6-1, and PU-6-6-2 after annealing at room temperature for one week are shown in Figure 3. The DSC thermal transition temperatures, endothermic peak temperatures and enthalpies of fusion are listed in Table IV. DSC thermal behavior is apparent in five temperature regimes. The soft segment glass transition temperature T_{g1} appears at -44, -33, -38 °C for PU-7-5, PU-6-6-1, and PU-6-6-2, respectively. T_{g1} values can be used as an indication of relative purity of the

soft segment domains. The more the soft segment domains are contaminated with the dissolved high glass transition temperature hard segments, the higher the soft domain T_{g1} [37]. The extent of hard segment/soft segment mixing depends on the overall hard segment content, both segment lengths, and the affinity of one segment for the other. The soft segment T_{g1} is also influenced by the restricted movement imposed at soft segment crystallization. The crystallites behaved as physical crosslinks; the high degree of soft segment crystallinity restricted the motion of soft segments and raised the soft segment T_{g1}. Since PU-6-6-1 had the highest and PU-7-5 had the lowest degrees of soft segment crystallinity, the T_{g1} of these polyurethanes decreased in the following sequence: PU-6-6-1 > PU-6-6-2 > PU-7-5.

The second region of interest is that corresponding to the melting of the soft segment (T_{m1}, around 11-56 °C). Comparing Tables III and IV, it is obvious that the polymerization of polyesterdiol with MDI and 1,4-butanediol leads to decreases of melting temperature T_{m1} and melting enthalpy ΔH_{m1} of polyester soft segments. The value of T_{m1} decreased in the following sequence: PU-6-6-1 > PU-6-6-2 > PU-7-5 and that of ΔH_{m1} decreased in the following sequence: PU-6-6-1 >> PU-7-5 ~ PU-6-6-2. The T_{m1} and ΔH_{m1} of the soft segment are indicators of degree of soft segments crystallinity [37]. These experimental results revealed that the degree of ordering the of polyester soft segment domain decreased in the following sequence: PU-6-6-1 > PU-6-6-2 > PU-7-5.

The remaining regions of DSC thermal behavior result from endotherms associated with hard segment domains. The endotherm around 52-88 °C (T_{m2} (I)) results from the breakup of hard segments with the short range ordering domain induced by room temperature annealing [9]. The endotherm around 120-175 °C (T_{m2}(II)) corresponds to the melting of the hard segment domain with long range ordering. The endotherm around 175-220 °C (T_{m2}(III)) corresponds to the melting of microcrystalline hard segments. From the DSC results, we found that PU-7-5 had long range ordering and microcrystalline hard segment domains with higher T_{m2}(II), ΔH_{m2}(II), T_{m2}(III) and ΔH_{m2}(III). However, no microcrystalline hard segment domains were observed for PU-6-6-1 and PU-6-6-2. PU-6-6-1 and PU-6-6-2 had long range and short range ordering hard segment domains with lower T_{m2}(I), ΔH_{m2}(I), T_{m2}(II), and ΔH_{m2}(II). Table IV and Figure 3 also show that PU-6-6-2 had higher T_{m2}(II) and ΔH_{m2}(II) than PU-6-6-1. In the present study, three PUs with similar weight fractions of soft segments were synthesized using the prepolymerization method, i.e. polyesters

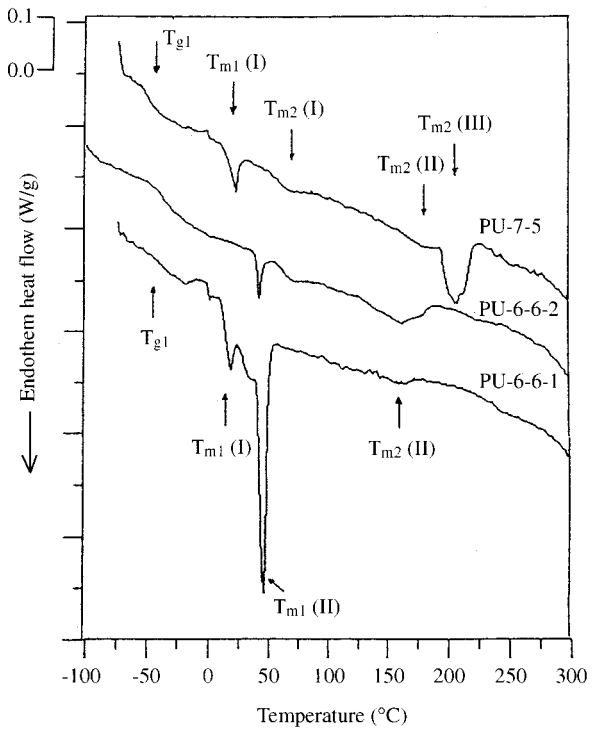

Figure 3. DSC curves of PU-7-5, PU-6-6-1, and PU-6-6-2.

were first reacted with MDI then chain extended with 1,4-butanediol. Thus soft and hard segments alternately linked to form a block copolymer. For PUs with a fixed soft segmental weight fraction and PU molecular chain length, the chain lengths of hard segments (copolymer of MDI and 1,4-butanediol) depends on the chain lengths of the soft segments. The PUs with longer soft segmental chain lengths should have fewer soft-hard block segmental repeat units. The hard segmental chain length is proportional to the total mole number of hard segmental monomers divided by the number of soft-hard block segmental repeat units. Thus for PUs with the same molecular weights, those with longer soft segmental chain lengths should have longer hard segmental chain lengths. Because PU-6-6-2 has shorter polyester molecular chain lengths, it had a shorter hard segmental chain length than PU-7-5 did. The shorter hard segmental chain length caused PU-6-6-2 to have a lower degree of hard segment crystallinity than PU-7-5 did. The DSC results showed that the degree of hard segment crystallinity increased in the following sequence: PU-6-6-1 < PU-6-6-2 < PU-7-5. The lower degree of hard segmental crystallinity of PU-6-6-1 compared to PU-6-6-2 will be discussed in the "*discussion section*".

2. Small angle X-ray scattering (SAXS) of PU

Small angle X-ray scattering involves the measurement of the scattering intensity as a function of

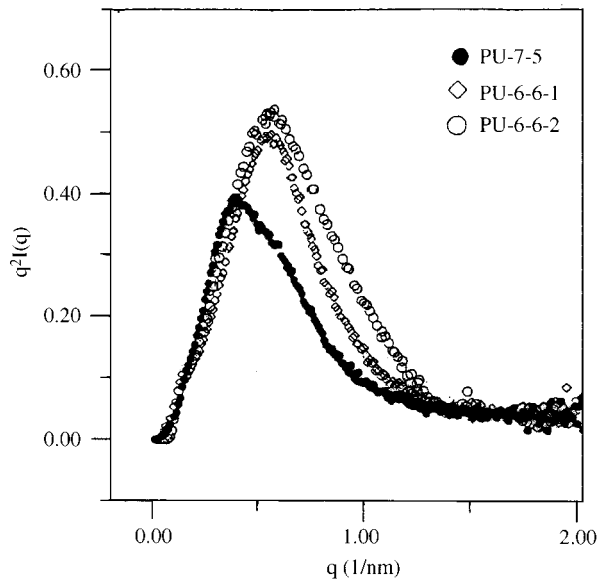

Figure 4. SAXS data $I(q)q^2$ versus q of PU-7-5, PU-6-6-1, and PU-6-6-2.

scattering angle. Scattering intensity arises due to local heterogenities in the electron density of the material. The inter-domain spacing, L, can be estimated from q_m corresponding to the maximum of $I(q)q^2$ *vs.* q curves using Bragg's equation [38]:

$$L = 2\pi/q_m \quad (1)$$

where $q = [4\pi \sin(\theta/2)]/\lambda$ is the scattering vector, θ the scattering angle, λ the wavelength, and $I(q)$ the scattering intensity at q. Typical SAXS intensity profiles ($I(q)q^2$ *vs.* q) for PU-7-5, PU-6-6-1, and PU-6-6-2 are shown in Figure 4. As shown in Figure 4, these profiles all exhibited a single scattering maximum, indicating average inter-domain spacing.

For systems with a lamellar structure, a one-dimensional correlation function $\gamma_1(r)$ will have a primary local maximum at a position r which corresponds to the inter-domain spacing, L_{1D}. The one-dimensional correlation function is shown as follows [38]:

$$\gamma_1(r) = \frac{1}{Q}\int_0^\infty q^2 I(q)\cos(qr)\,dq \quad (2)$$

where Q is the invariant and can be obtained by integrating $I(q)q^2$ over all the range of scattering angles.

$$Q = \int_0^\infty q^2 I(q)\,dq \quad (3)$$

Typical correlation functions $\gamma_1(r)$ of these polyurethanes are shown in Figure 5. The periodicity, L_{1D}, can be estimated from the position of the first subsidiary maximum in these correlation functions. The inter-domain spacing, L and L_{1D}, are listed in Table V. The results of Figures 4 and 5 showed that PU-6-6-1 and PU-6-6-2 had similar L (or L_{1D}) values, but the L (or L_{1D}) values of PU-6-6-1 and PU-6-6-2 were shorter than those for PU-7-5.

Table V. SAXS lamellar repeat distances of polyurethanes annealed at room temperature.

Polyurethane	PU-7-5	PU-6-6-1	PU-6-6-2
L (nm) (from invariant Q)	17.2	11.7	11.2
L_{1D} (nm) (from γ_{1D})	18.4	11.3	11.4

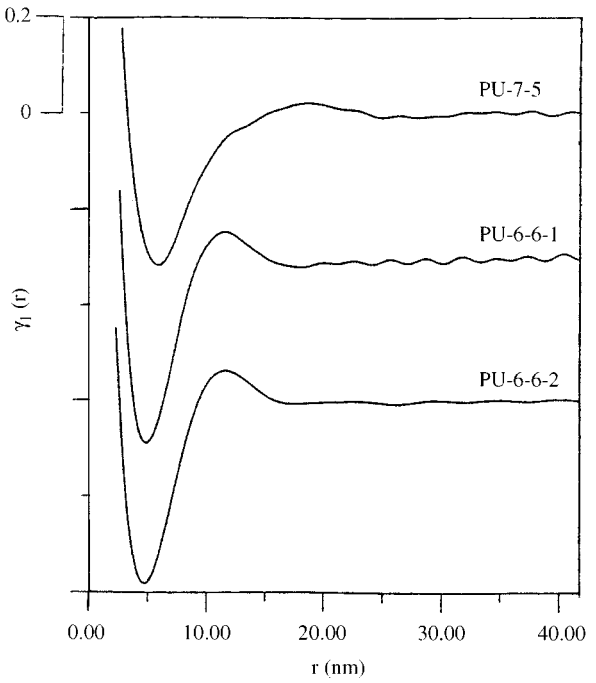

Figure 5. One dimensional correlation functions $\gamma_1(r)$ of PU-7-7, PU-6-6-1, and PU-6-6-2.

For polyurethane containing amorphous soft segments with crystalline hard segments dispersed in the amorphous soft domain, the X-ray scattering is contributed mainly by the hard segments (the aromatic hard segments had a higher electron density than the aliphatic soft segments). However, for polyurethanes containing crystalline soft segments with amorphous hard segments, the X-ray scattering comes mainly from the crystalline soft segments with a higher electron density. Figure 6 shows the graph of the morphology of PU. This graph indicates that the average inter-domain spacing (L or L_{1D}) of SAXS depends on (1) the molecular chain length of the polyester segments, (2) the molecular chain length of the hard segments, (3) the number and sizes of

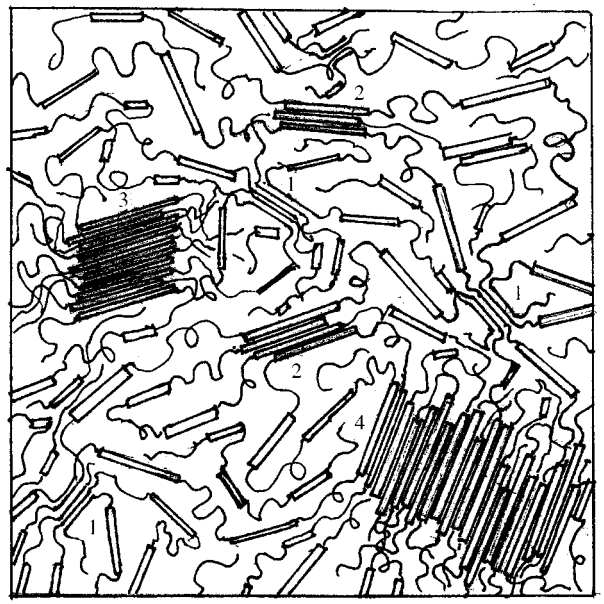

Figure 6. Morphology of polyurethane. (∿) soft segments, (=) hard segments, (1) soft segment ordering domain, (2) short range ordering hard segment domain, (3) long range ordering hard segment domain, and (4) microcrystalline structure of hard segments.

soft segmental crystallites, and (4) the number and sizes of hard segmental crystallites. A shorter polyester molecular chain length would cause a shorter inter-domain spacing between the hard-hard or soft-soft domains. Thus for polyurethanes with a similar degree of soft and hard segmental crystallinity and crystallite sizes, those with shorter soft segment molecular chain lengths should have shorter inter-domain spacing L (or L_{1D}). For PUs with the same soft and hard segmental molecular chain lengths, those with lower degrees of crystallinity (or smaller crystallite sizes or higher crystallite particle numbers) should have shorter inter-domain spacing.

Since PU-6-6-1 and PU-7-5 had similar polyester soft segment molecular chain lengths, the difference in the L (or L_{1D}) values between these two polyurethanes depends on the hard and soft segmental crystallite sizes and particle numbers. However, the polyester soft segment chain length of PU-6-6-2 was shorter than those of PU-6-6-1 and PU-7-5; the difference in the L (or L_{1D}) values between PU-6-6-2 with PU-6-6-1 or PU-6-6-2 with PU-7-5 depended not only on the hard and soft segmental crystallite sizes and crystallite particle numbers but also on the polyester soft segmental chain lengths. The melting temperature T_m and melting enthalpy ΔH_m are indicators of crystallite sizes and degree of crystallinity, respectively. A larger crystallite size would cause a higher T_m. The value of ΔH_m is proportional to the product of crystallite sizes and crystallite particle numbers. From the DSC data, we know that PU-6-6-1 had a very high degree of soft segment crystallinity (ΔH_{m1} = 34.8 J/g) and a low degree of hard segment crystallinity (ΔH_{m2} = 3.2 J/g), while PU-7-5 had a low degree of soft segment crystallinity (ΔH_{m1} = 4.2 J/g) and a medium degree of hard segment crystallinity ($\Delta H_{m2}(II) + \Delta H_{m2}(III)$ = 19.0 J/g). Both the crystallized soft and hard segments might have contributed to the X-ray scattering. The L (or L_{1D}) was an average distance between the soft and hard segment ordering domains. The shorter L (or L_{1D}) of PU-6-6-1 compared to that of PU-7-5 could be due to the very high degree of soft segment crystallinity of PU-6-6-1, which reduced the size of the disordering domains and thus reduced the distance between the ordering domains.

The DSC data showed that PU-6-6-2 ($T_{m1}(II)$ = 43 °C, ΔH_{m1} = 2.0 J/g for soft segments and $T_{m2}(I)$ = 71 °C, $\Delta H_{m2}(I)$ = 2.1 J/g, $T_{m2}(II)$ = 162 °C, $\Delta H_{m2}(II)$ = 8.6 J/g for hard segments) had a much lower degree of soft segment crystallinity than PU-6-6-1 ($T_{m1}(II)$ = 46 °C, $T_{m1}(I)$ = 19 °C, $\Delta H_{m1}(I+II)$ = 34.8 J/g) and a lower degree of hard segment crystallinity and smaller crystallite sizes than PU-7-5 ($T_{m2}(II)$ = 162 °C, $T_{m2}(III\text{-}a)$ =185 °C, $T_{m2}(III\text{-}b)$ = 198 °C, $\Delta H_{m2}(II+III)$ = 19.0 J/g). Thus the overall soft and hard segment crystallite sizes and degree of crystallinity of PU-6-6-2 were between those of PU-6-6-1 and PU-7-5. If these three polyurethanes had similar polyester soft segment molecular chain length, then the L (or L_{1D}) value of PU-6-6-2 should be between those of PU-6-6-1 and PU-7-5. However, the shorter polyester soft segmental molecular chain length (which also resulted in a shorter hard segment molecular chain length) caused PU-6-6-2 to have an L (or L_{1D}) shorter than that of PU-7-5 but similar to that of PU-6-6-1 (because PU-6-6-1 had a much higher degree of soft segmental crystallinity).

3. FTIR study

Almost all of the infrared research on PU has been focused on two principal vibrational regions: the N–H stretching vibration (3200-3500 cm^{-1}) and the C=O stretching vibration amide-I region (1637-1730 cm^{-1}) [39-46]. In this investigation, FTIR was used to study the effect of polyester crystallinity on the hydrogen bonding behavior of PU. The infrared spectra for PU-6-6-1, PU-6-6-2, and PU-7-5 annealed at room temperature are shown in Figure 7. Figure 8 illustrates the infrared spectra of N–H and the C=O stretching vibrations of these polyurethanes. There are distinct differences between the spectra at N–H stretching and at the C=O stretching regions with different degrees of hard segmental and polyester soft segmental crystallinity, due mainly to peak shifts and intensity changes.

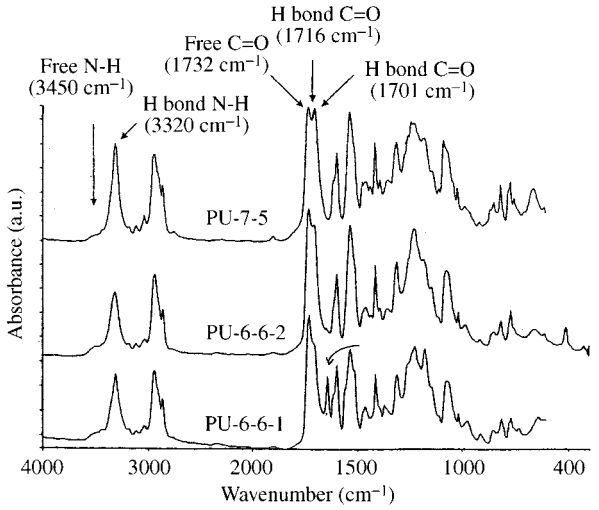

Figure 7. FTIR spectra of PU-7-5, PU-6-6-1, and PU-6-6-2.

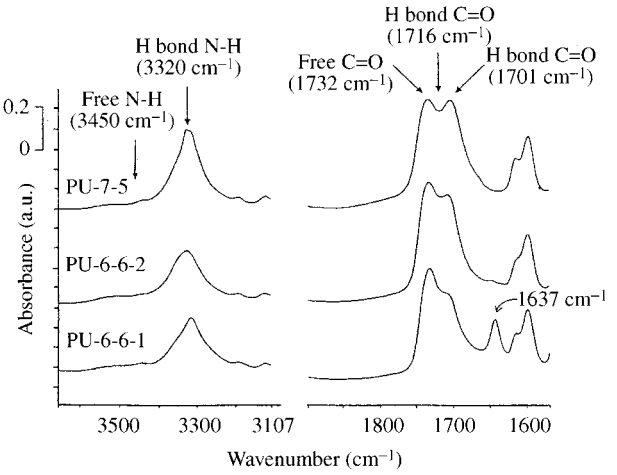

Figure 8. FTIR spectra of N-H and C=O stretching vibrations of PU-7-5, PU-6-6-1, and PU-6-6-2.

It is well-known that the infrared absorbance of H-bonded urethane carbonyl appears at lower wave numbers than that of free urethane carbonyl [41-43]. The amide-I infrared spectra of semi-crystalline samples such as nylons [44] and polyurethanes [45] have been reported to comprise distinct spectral features due to the degree of carbonyl H-bonding. In order of increasing wave numbers, these are H-bonded carbonyl groups in ordered ("crystalline") soft domains (1624-1656 cm^{-1}), H-bonded carbonyl groups in ordered ("crystalline") hard domains (1699-1706 cm^{-1}), H-bonded carbonyl groups in disordered ("amorphous") conformations (1714-1718 cm^{-1}), and non-H-bonded (free) carbonyl groups (1731-1733 cm^{-1}). Similarly, two distinct bands are observed in the N–H stretching region, i.e., 3320-3329 and 3441-3450 cm^{-1}, which are attributed to H-bonded and "free" N–H stretching vibrations, respectively [46]. As shown in Figures 7 and 8, the IR spectrum of PU-6-6-1 exhibited three C=O amide-I bands, i.e., strong free carbonyl stretching (1732 cm^{-1}), weak shoulder H-bonded carbonyl stretching in hard domains (1701 cm^{-1}), and a medium H-bonded carbonyl stretching in soft domains (1637 cm^{-1}). Only two C=O amide-I stretching bands were observed in the IR spectra of PU-6-6-2 and PU-7-5, i.e., strong free carbonyl stretching (1732 cm^{-1}) for both polyurethanes, a medium H-bonded carbonyl stretching in hard domains (1701 cm^{-1}) for PU-6-6-2, and a strong H-bonded carbonyl stretching in hard domains (1701 cm^{-1}) for PU-7-5. Skrovank et al. [44], using FTIR, studied H-bond formation of nylon-11. Their results showed three amide-I carbonyl stretching bands, i.e. free carbonyl groups (1680 cm^{-1}), H-bonded carbonyl groups in disordered conformation ("amorphous") (1656 cm^{-1}), and H-bonded carbonyl groups in ordered conformation ("crystalline") (1638 cm^{-1}). Interestingly, the peak frequency of H-bonded carbonyl stretching in the ordered domains (1638 cm^{-1}) of nylon-11 is very close to that of H-bonded carbonyl stretching in the soft domains (1637 cm^{-1}) of PU-6-6-1. Since nylon-11 is an aliphatic polyamide, we believe that the –C=O stretching at 1637 cm^{-1} of PU-6-6-1 was due to the H-bonded –C=O formed from the –NH of urethane and –C=O of polyesters. No –C=O stretching at 1637 cm^{-1} was observed for PU-6-6-2, indicating that no H-bond formed between the hard segmental –NH and soft segmental –C=O groups. It is obvious that the trapping and dispersing of hard segments inside the soft ordered domain caused the H-bond formation through hard segmental –NH and soft segmental –C=O groups in PU-6-6-1.

The H-bonded N–H stretching frequency does not exhibit separate features attributable to ordered and disordered H-bonded conformations but rather reflects the overall distribution of H-bonded strength. In Figure 8, the peak height of the 1701 cm^{-1} absorbance band decreased in the following sequence: PU-7-5 > PU-6-6-2 > PU-6-6-1. Similar behavior was also observed in the absorbance band of the N–H stretching vibration, i.e., the free –NH stretching absorbance band at 3450 cm^{-1} increased in the following sequence: PU-7-5 < PU-6-6-2 < PU-6-6-1, indicating the degree of hard segmental H-bonding decreased sequentially from PU-7-5 to PU-6-6-2 then PU-6-6-1.

4. Discussion

The morphology of polyurethanes depends on the following factors: (1) the compatibility of the soft and hard segments; (2) the polyester soft seg-

mental chain length; (3) the geometric fits of soft-to-soft segments, soft-to-hard segments, and hard-to-hard segments; and (4) the mobility of hard segments inside the soft domain [14,15]. Since the repeat units of polyester-6-6 and polyester-7-5 had the same molar fraction of the –COO group, these two polyesters should have the same solubility parameters. The compatibility of PU hard segments with soft segments should be similar for all PUs. Under the same processing conditions and thermal history, the morphology of PUs should depend on factors (2), (3), and (4). PUs polymerized from polyester soft segments with longer molecular chains should result in longer hard segmental chain lengths. From the thermodynamic point of view, PUs with longer soft and hard segmental chains should have a higher degree of soft and hard segmental phase segregation. As a result of annealing the PU at a temeprature higher than the T_g of the hard segments (around 80 °C), the soft segments behaved like flexible coils while the hard segments behaved like rigid chains. The mobility of the hard segments inside the soft-domain decreased with increasing hard segmental chain length. Increasing the mobility of hard segments increases the chance of the hard segments moving out from the soft domain and forming ordered hard segment domains through –NH···O=C– hydrogen bonds. From a kinetic point of view, increaing the hard segmental chain length caused a decrease in hard segmental mobility leading to a decrease in the degree of hard segmental crystallinity.

Another factor controlling the phase segregation of soft and hard segments is the geometric structure of soft and hard segments. Figure 1 shows the geometric structures of "*MDI+1,4-butanediol*" hard segments, polyester-6-6, and polyester-7-5. Since all the PUs had hard segments consisting of even carbon monomers, it is obvious that PU-6-6 had a better hard-to-soft geometric fit than PU-7-5. Figure 1 also shows that the polyester "*zig-zag*" structure caused PU-6-6 to have a better soft-to-soft geometric fit than PU-7-5.

The polyester soft segments of PU-6-6-1 and PU-7-5 have a similar molecular weight distribution. The difference in morphology between these two PUs depends on the hard-to-soft segmental geometric fit. Becase of the better hard-to-soft segmental geometric fit while the PU was cooled from 230 °C to a temperature above T_g of hard segments, PU-6-6-1 formed fewer hard-to-hard segmental –NH···O=C hydrogen bonds than PU-7-5 did. When PU was annealed at a temperature below T_{m1} of soft segments, because of the better soft-to-soft geometric fit, PU-6-6-1 had a higher degree of polyester soft segmental crystallization than PU-7-5 did. The DSC data

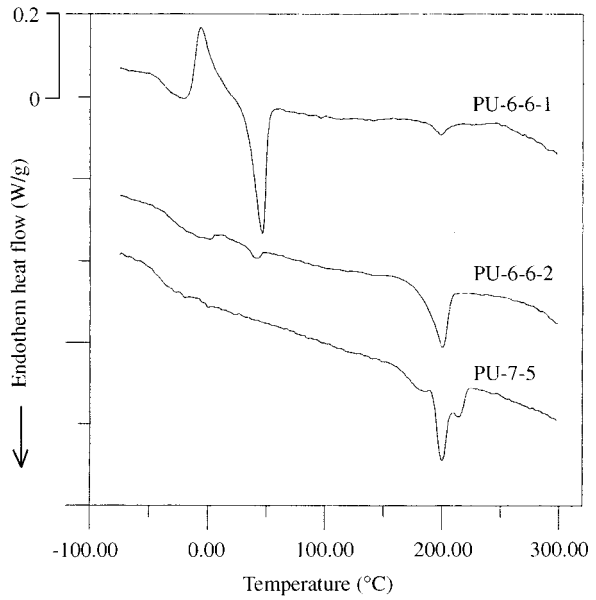

Figure 9. DSC curves of PU-6-6-1, PU-6-6-2, and PU-7-5 after annealing at 150 °C for 48 hr then quenched to -80 °C with liquid nitrogen.

revealed that PU-6-6-1 had a higher degree of soft-segment crystallinity while PU-7-5 had a higher degree of hard-segmental crystallinity. FTIR data showed that only PU-6-6-1 had –C=O stretching at 1637 cm^{-1}, indicating the trapping and dispersing of hard segments inside the polyester soft segmental ordered domain.

Since PU-6-6-1 and PU-6-6-2 had the same soft segment chemical structures and soft segment contents but different soft segmental molecular chain lengths, these two polyurethanes had similar soft and hard segmental compatibility and a similar soft-to-hard segemental geometric fit. The difference in morphology of these two polyurethanes depends on the soft and hard segmental molecular chain lengths. The soft segment molecular weight of PU-6-6-1 was higher than that of PU-6-6-2; thus PU-6-6-1 consisted of longer soft and hard segmental chain lengths, i.e., a lower number of soft-hard block repeat units. Owing to the longer hard segmental chain length, at a temperature higher than hard segmental T_g the mobility of hard segements inside the soft domain was slower for PU-6-6-1 than for PU-6-6-2. When PU was cooled from 230 °C to a temperature above T_g of hard segments, PU-6-6-1 exhibited fewer hard segments moving out from the soft domain and thus a lower degree of hard segemental crystallinity than PU-6-6-2. Athough both PU-6-6-1 and PU-6-6-2 had been annealed at 150 °C for 48 hr, the degree of hard segmental crystallinity of PU-6-6-1 was still much lower than that of PU-6-6-2 (Figure 9). Thus in the present case, kinetic control was the key

factor in hard segmental crystallization. As the PU was cooled froom 230 °C to a temperature below T_g of the hard segments, hard segmental crystallite formed in PU-6-6-2 but very few crystallites formed in PU-6-6-1. Since the hard segmental crystallites acted as physical crosslinks and restricted the motion of the soft segments, the mobility of the soft segments was lower for PU-6-6-2 than for PU-6-6-1 when they were annealed at room temperature. Since PU-6-6-1 had a higher soft segmental mobility at room temperature and a higher soft segmental molecular weight, both kinetics and thermodynamics favored PU-6-6-1 having a higher degree of soft segmental crystallinity. Our experimental results revealed that PU-6-6-1 had a higher degree of soft segmental crystallinity and a lower degree of hard segment ordering than PU-6-6-2 had.

The morphological difference between PU-6-6-2 and PU-7-5 depends on (1) soft-to-soft and hard-to-soft segmental geometric fit and (2) soft and hard segmental molecular chain lengths. The polyester soft segments containing even carbon monomers had a better soft-to-soft geometric fit and thus a higher degree of soft segmental crystallinity. Though PU-6-6-2 had a shorter polyester soft segmental chain length than PU-7-5 did, the better soft-to-soft geometric fit of PU-6-6-2 led it have a similar degree of soft segment crystallinity as PU-7-5 did (DSC data ΔH_{m1}(I+II) = 2.0 and 4.2 J/g for PU-6-6-2 and PU-7-5, respectively). The higher polyester soft segment molecular chain length and worse soft-to-hard segmental geometric fit resulted in a higher degree of soft and hard segment phase segregation. PU-7-5 (odd carbon monomer soft segments with even carbon monomer hard segments) had a worse soft-to-hard segmental geometric fit and higher polyester molecular chain length than PU-6-6-2 (even carbon monomer soft segments with even carbon monomer hard segments); thus PU-7-5 had a higher degree of hard segment crystallinity than PU-6-6-2.

Conclusion

In this study, using DSC, FTIR, and SAXS, we showed the morphology of polyester-based polyurethane was strongly affected by (1) the polyester soft segmental chain length; (2) the geometric fits of soft-to-soft segments, soft-to-hard segments, and hard-to-hard segments; and (3) the mobility of hard segments inside the soft domain.

Acknowledgement

The authors would like to express their gratitude thanks for the financial support of the National Science Council of ROC through grant NSC 88-2216-E-155-004.

References

1. S. L. Cooper and A. V. Tobolsky, *J. Appl. Polym. Soc.*, **10**, 1837 (1966).
2. T. K. Kwei, *J. Appl. Polym. Sci.*, **27**, 2891 (1982).
3. D. S. Huh and S. L. Cooper, *Polym. Eng. Sci.*, **11**, 369 (1971).
4. C. E. Wilkes and C. S. Yusek, *J. Macromol. Sci. Phys.*, **B7**, 157 (1973).
5. (a) G. G. Jr. Seefried, J. V. Koleske and F. E. Critchfield, *J. Appl. Polym. Sci.*, **19**, 2493 (1975); (b) *ibid.*, **19**, 3185 (1975).
6. G. W. Miller and J. H. Saunders, *J. Polym. Sci.*, **A-18**, 1923 (1970).
7. S. Abouzahr and G. L. Wilkes, *J. Appl. Polym. Sci.*, **29**, 2695 (1984).
8. J. A. Miller, S. B. Lin, K. K. S. Hwang, K. S. Wu, P. E. Gibson and S. L. Cooper, *Macromolecules*, **18**, 32 (1985).
9. R. W. Seymour and S. L. Cooper, *Macromolecules*, **6**, 48 (1973).
10. J. T. Koberstein and T. P. Russell, *Macromolecules*, **19**, 714 (1986).
11. J. T. Koberstein and A. F. Galambos, *Macromolecules*, **25**, 5618 (1992).
12. J. T. Koberstein, A. F. Galambos and L. M. Leung, *Macromolecules*, **25**, 6195 (1992).
13. J. T. Koberstein and L. M. Leung, *Macromolecules*, **25**, 6205 (1992).
14. Y. Li, T. Gao and B. Chu, *Macromolecules*, **25**, 1737 (1992).
15. Y. Li, T. Gao, J. Liu, K. Linliu, C. R. Desper and B. Chu, *Macromolecules*, **25**, 7365 (1992).
16. Y. Li, J. Liu,H. Yang, D. Ma and B. Chu, *J. Polym. Sci., Polym. Phys., Ed.*, **31**, 853 (1996).
17. Y. Li, W. Kang, J. O. Staffer and B. Chu, *Macromolecules*, **27**, 612 (1994).
18. R. J. Goddar and S. L. Cooper, *J. Polym. Sci., Polym. Phys. Ed.*, **32**, 1557 (1994).
19. B. P. Grady, E. M. O'Connell, C. Z. Yang and S. L. Cooper, *J. Polym Sci., Polym. Phys. Ed.*, **32**, 2357 (1994).
20. R. J. Goddar and S. L. Cooper, *Macrromolecules*, **28**, 1401 (1995).
21. N. J. Clayden, C. Nijis and G. Eeckhaut, *Macromolecules*, **31**, 7820 (1998).
22. D. J. Martin, G. F. Meijs, P. A. Gunatillake, S. J. McCarthy and G. M. Renwick, *J. Appl. Polym. Sci.*, **64**, 803 (1997).
23. S. C. C. Paik, C. B. Hu and C. S. Wu, *Macromolecules*, **13**, 111 (1980).
24. J. A. Miller and S. L. Cooper, *J. Polym. Sci., Polym. Phys. Ed.*, **23**, 1065 (1985).
25. L. M. Leung and J. T. Koberstein, *Macromolecules*, **19**, 706 (1986).
26. J. T. Koberstein and I. Gancarz, *J. Polym. Sci., Polym. Phys. Ed.*, **24**, 2487 (1986).
27. J. C. West and S. L. Cooper, *J. Polym. Sci., Polym. Symp.*, **60**, 27 (1977).
28. M. M. Coleman, K. H. Lee, D. J. Skrovanek and D. C. Painter, *Macromolecules*, **19**, 2149 (1986).

29. R. J. Goddar and S. L. Cooper, *Macromolecules*, **28**, 1390 (1995).
30. H. J. Tao, C. W. Meuse, X. Yang, W. J. MacKnight and S. L. Hsu, *Macromolecules*, **27**, 7146 (1994).
31. L. A. Gower and D. J. Lyman, *J. Polym. Sci., Polym. Chem., Ed.*, **33**, 2257 (1995).
32. G. L. Wilkes, S. L. Samuel and R. G. Crystal, *J. Macromol. Sci.-Phys.*, **B10**, 203 (1974).
33. J. Foka and H. Janik, *Polym. Eng. Sci.*, **29**, 113 (1989).
34. S. L. Chang, T. L. Yu, C. C. Huang, W. C. Chen, K. Linliu and T. L. Lin, *Polymer*, **39**, 3479 (1998).
35. Y. Camberlin and J. P. Pascault, *J. Polym. Sci., Polym. Phys. Ed.*, **22**, 1835 (1984).
36. J. H. Saunders and K. C. Frisch, *Polyurethanes Chemistry and Technology*, Part **I**, Interscience Publishers, New York, 1962, chap. 6.
37. T. R. Hesketh, J. W. C. van Bogart and S. L. Cooper, *Polym. Eng. Sci.*, **20**, 190 (1980).
38. D. Tyagi, J. E. McGrath and G. L. Wilkes, *Polym. Eng. Sci.*, **26**, 1371 (1986), and references in there.
39. D. J. Skrovanek, S. E. Howe, P. C. Painter and M. M. Coleman, *Macromolecules*, **18**, 1676 (1985).
40. F. Papadimtrakopoulos, E. Sawa and W. J. MacKnight, *Macromolecules*, **25**, 4682 (1992).
41. M. M. Coleman, K. H. Lee, D. J. Skrovanek and P. C. Painter, *Macromolecules*, **19**, 2149 (1986).
42. R. W. Seymour, G. M. Estes and S. L. Cooper, *Macromolecules*, **3**, 579 (1970).
43. W. J. MacKnight and W. J. Yang, *J. Polym. Sci., Polym. Symp.*, **42**, 817 (1973).
44. D. J. Skrovanek, P. C. Painter and M. M. Coleman, *Macromolecules*, **19**, 699 (1986).
45. S. K. Pollack, D. Y. Shen, S. L. Hsu, Q. Wang and H. D. Stidham, *Macromolecules*, **22**, 270 (1988).
46. F. C. Wang, M. Feve, T. M. Lam and J. P. Pascault, *J. Polym. Sci., Polym. Phys. Ed.*, **32**, 1305 (1994).